



Preparation of Thermal Active Nano-Materials for Application in Water Desalination and Wastewater Treatment, Dielectric Study

M. A. El-Khateeb,^{a*} Mehrez El-Naggar,^b Ragab Mahani^c, M. A. Salem^d

^a National Research Centre, Institute of Environmental Research, Water Pollution Research Dept., 33 El Behouth St., Dokki, Giza, 12622, Egypt, elkateebcairo@yahoo.com

^b National Research Centre, Textile Research and Technology Institute, 33 El Behouth St., Dokki, Giza, 12622, Egypt, mehrez_chem@yahoo.com

^c National Research Centre, Institute of Physics Research, Microwave Physics and Dielectrics Dep., Dokki, Giza, 12622, Egypt, rmsoliman66@yahoo.com

^d National Research Centre, Institute of Physics Research, Solid State Physics Dept., Dokki, Giza, 12622, Egypt, masalem11@yahoo.com



CrossMark

Abstract

Egypt has recently experienced a severe water deficit for a variety of applications. This situation can become worse very soon. Consequently, it is critical to value the non-traditional water supply. The current study aims to prepare a floating membrane using polyvinyl alcohol (PVA), carboxymethyl cellulose (CMC) polymer, and copper oxide (CuO) for water desalination. The possibility of using the resulting membrane to distillate water with brine made using sodium chloride salt was tested. The prepared floating membrane was found to be effective in desalinating water. In addition, CMC/PVA- based composites have been electrically investigated to determine the low delay characteristics of high-frequency signal transmission. Using a wideband dielectric spectrometer and a wide frequency range (10-1-106 Hz), these composites' permittivity and loss tangent were investigated (BDS). Experimental results reported low permittivity (~4 to 5) and loss tangent (~0.0006 to ~0.0009) values. These features would make the composites promising in the high-frequency applications and desalination of saline water.

Keywords: CMC/PVA, CuO, Permittivity, Loss tangent

1. Introduction

Energy and water are essential components for life, economic growth, and societal advancement. The Earth's ability to support humanity in the near future will be severely tested, notably in terms of the essential resources of clean water and energy supply [1, 2]. The situation has become even worse with the significant surge in energy prices [3, 4]. Water desalination has taken on a greater significance as a technique of supplying fresh water to a thirsty world due to the depletion of surface and subterranean freshwater resources and rising water needs. Traditional desalination methods either use the energy-intensive distillation process or the polymeric membrane filtration method, which demands high freshwater flux and salt rejection rates [3, 5, 6].

Through photovoltaic, photochemical, and photothermal processes, respectively, solar energy can be captured and transformed into a variety of energy types, including electricity, chemical (fuels), and

thermal energy. A sustainable way to reduce the drinking water crisis is to utilize solar energy to distill salty or contaminated water to produce clean water. Solar energy is a green, renewable energy source [7, 8]. In order to address the growing demand for solar water evaporation applications, the development of suitable photothermal conversion materials during solar energy harvest has attracted an increasing level of interest [9, 10]. With the addition of materials to its matrix, solar systems' poor photothermal efficiency was partially improved. These materials aid in the increased absorption of solar energy, but the water's overall photothermal efficiency is reduced by the ineffective process of heat transfer from the coating's surface [11, 12]. Inorganic materials like semiconductors and noble metals as well as organic materials like conjugated polymers, dyes, and carbon-based materials can exhibit these materials [12]. A new strategy to use solar energy for a variety of purposes, including steam generation, domestic water

*Corresponding author e-mail: elkateebcairo@yahoo.com.; (M. A. El-Khateeb).

Receive Date: 10 April 2022, **Revise Date:** 09 May 2022, **Accept Date:** 16 May 2022, **First Publish Date:** 16 May 2022

DOI: 10.21608/EJCHEM.2022.132647.5861

©2022 National Information and Documentation Center (NIDOC)

heating, distillation, desalination, purification, and photothermal catalysis, is to use nano-structured materials as heat producers for gathering solar illumination [11, 12]. One benefit of the photothermal effect caused by nanostructured materials is its ability to precisely modulate heat to a specific location at the nanoscale. Additionally, nanomaterials exhibit localized surface plasmonic resonance, quantum confinement effects, and other fascinating phenomena because of their distinctive electrical and optical properties. Photothermal functions are favoured by all of these characteristics, as well as a wide surface area, programmable surface properties, and customizable structures. Both the efficiency of sunlight's thermal energy conversion and its absorption are factors in the development of effective solar thermal collector materials [12, 13].

The blending of polymers can result in producing materials with enhanced properties more rapidly compared to developing new polymer chemistry. In order to optimize light harvesting efficiency and consequently increase the production of heat energy, a variety of photothermal materials, including plasmonic metals, carbon-based materials, and polymers with broadband absorption, have been thoroughly explored [14, 15]. The current study aims to produce a floating membrane using polyvinyl alcohol (PVA), carboxymethyl cellulose (CMC) polymer, and copper oxide (CuO) for water desalination. Water desalination efficiency and porosity of these materials have been correlated.

2. Materials and methods

2.1. Materials

Sigma Aldrich provided sodium hydroxide, copper nitrate, and polyvinyl alcohol (PVA). The carboxymethyl cellulose (CMC) polymer was purchased from the Chinese company Kelong Chemical Factory.

2.2. Methods

2.2.1 Synthesis of CuO nanoparticles

Copper nitrate ($\text{Cu}(\text{NO}_3)_2 \cdot 3\text{H}_2\text{O}$) was used in the precipitation process to create copper oxide (CuO) nanoparticles. In deionized water, 0.1 M of copper nitrate solution was made, then 0.1 M of sodium hydroxide (NaOH) solution was added gradually while being vigorously stirred up until pH 14, where a black precipitate developed. Until pH 7 was achieved, the precipitate was repeatedly washed with 100% ethanol and deionized water. The cleaned precipitate

underwent 16 hours of drying at 80 °C and 4 hours of calcination at 500 °C. After that, 0.08 g of the net-produced powder was dissolved in 25 mL of deionized water and stirred with a magnetic stirrer for 30 minutes at room temperature [16].

2.2.2 Preparation of CMC/PVA/CuO bionanocomposites

Different PVA/CMC/CuO nanocomposites were manufactured via solution casting techniques. Firstly, PVA and CMC solutions (5% w/v) were prepared individually and then mixed at the ratio of 1:1 (v/v). Different concentrations of the as-prepared CuO-NPs (4 mL, 8 mL and 12 mL) were added to various solutions of the PVA/CMC solution and kept under a mechanical stirrer for 15 min. Distinctly, tannic acid (TA) (2% wt./wt. of polymer blend) was sonicated with CuO-NPs to license good dispersion of nanomaterials. Then, the TA with CuO-NPs is added to the polymer blend with continuous mechanical stirring. After that, the mixture was cured at 100°C for 10 minutes to make the blend cross-linked. The solution was then allowed to cool until it reached room temperature. The PVA/CMC/CuO nanocomposites solutions were transferred into a transparent glass petri dish and left at room temperature for 72 h in order to vaporize the solvent, then create the PVA/CMC/CuO bionanocomposites membrane. The fabricated membranes were coded as CMC-C0, CMC-C4, CMC-C8 and CMC-C12 states, to the concentration of the utilized CuO-NPs with CA, where CMC-C0 signifies the preparation of CMC/PVA membrane without CuO-NPs. On the other hand, CMC-C4, CMC-C8 and CMC-C12 refer to the preparation of CA membrane blended with 4 mL, 8 mL and 12 mL of CuO-NPs, respectively.

2.2.3 Characterization

- Transmission Electron Microscopy

Using a transmission electron microscope (TEM) model JEM-1230 from Japan, operated at 120 kV, with a maximum magnification of 600×10^3 and a resolution of 0.2 nm, the morphology of the samples of manufactured nanocomposites was investigated. Additionally, the morphology of the generated CuO-NPs was created by drying a drop of the solution on a copper grid that had been coated with carbon using the Joel-100S transmission electron microscope, which has a resolution of 0.3 nm.

- Dielectric Spectroscopy

At room temperature, measurements of the dielectric properties of CMC/PVA loaded with 8 mL of CuO were made across a broad frequency range (10^1 - 10^6 Hz). The mixed sample was placed between two electrodes of a measurement cell linked to an Impedance/Gain-Phase Analyzer 1260 to achieve this.

Permittivity (ϵ'), dielectric loss (ϵ''), and AC conductivity (σ_{ac}) are the three dielectric qualities that are of interest in this context. The following relations can be used to provide these features [17]:

$$\epsilon' = C \frac{d}{\epsilon_0 A} \quad (1)$$

$$\epsilon'' = \epsilon' \tan \delta \quad (2)$$

$$\sigma_{ac} = \omega \epsilon_0 \epsilon'' \quad (3)$$

where $\epsilon_0 = 8.85 \times 10^{-12}$ F/m is the vacuum permittivity, $\omega (= 2\pi f)$ is the angular frequency, f is the frequency of the electric field in Hertz, and $\tan \delta (= \epsilon''/\epsilon')$ is the loss tangent or dissipation factor, C is the capacitance of the measured sample in Farad, d is the thickness of the sample in meter, and A is the sample surface area.

3. Results and discussion

3.1. Particle shape of CuO-NPs using TEM

The TEM micrographs of the created CuO-NPs at low and high magnifications are displayed in (Figure 1 a, b). It is evident that the CuO-NPs that have been synthesized have a uniformly spherical shape and a nanosize of roughly 10-15 nm. However, a small number of CuO-NPs aggregates were found indicating that certain interfacial tensions between precursor particles created by OH- bonding were diminished during the curing process of the obtained CuO-NPs.

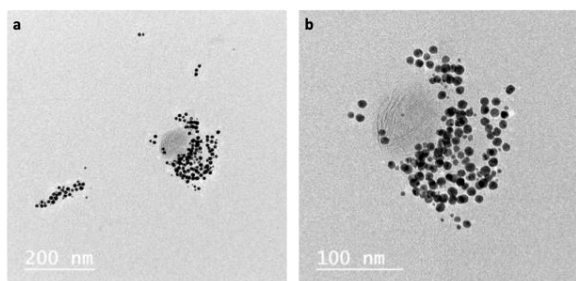


Figure 1: (a, b) TEM images of the as-prepared CuO-NPs at low and high magnifications

3.2. Morphology of the produced membrane loaded with Cu-NPs using SEM

The SEM was utilized to examine the morphological features of the produced membranes. It is observed that the membrane based on CMC/PVA composite is composed of a porous structure and the surface appears as a rough surface as detected in Figure 2 (a). Upon mixing the composite with 4 mL of Cu-NPs, the surface is changed with the appearance of particles on the surface of the prepared film (Figure 2 b). On the contrary, upon increasing the concentration of CuO-NPs to 8 mL and 12 mL as displayed in Figures 2 (c, d) respectively, the surface became significantly changed. The surface appears to be smooth with the appearance of huge particles of CuO-

NPs deposited onto the surface in easily entering the pores of the composite membrane. The available porous structure is mainly affected by the deposited amount of the utilized CuO-NPs.

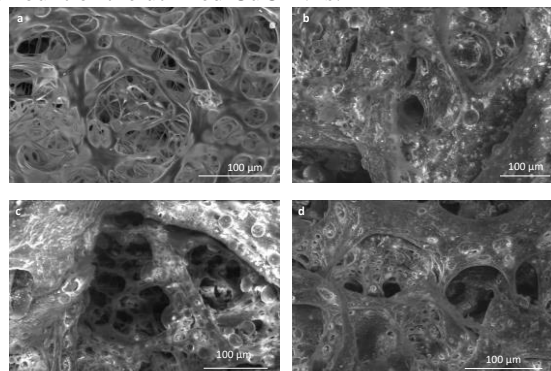


Figure 2: The SEM of (a) CMC-C0, (b) CMC-C-4, (c) CMC-C-8 and (d) CMC-C-12

3.3. Desalination using floating membranes

The received solar energy is absorbed by the solar absorber (combined with the floating membrane), and then converted into heat energy, which is used to heat water into steam [18]. Synthetic saline water was prepared by dissolving 10 g/l NaCl. Table 1 shows the evaporation rate for the used membrane samples as affected by direct sunlight. The volume of water was 500 ml.

Table 1: The rate of water desalination using the floating membrane

Time (h)	Blank	Sample with floating membrane
2	--	4 ml
4	4 ml	8 ml
6	7 ml	14 ml
8	8 ml	19 ml
10	10 ml	42 ml
24	18 ml	87 ml
48	120 ml	180 ml

The experiment was extended from 7 am to 5 pm during the period from 3/3/2021 to 6/3/2021.



Figure 3: Water evaporation of saline water, and the corresponding thermal picture

3.4. Dielectric spectroscopy

The frequency dependence of permittivity (ϵ') and the loss tangent ($\tan\delta$) as well as AC conductivity (σ_{ac}) for the CMC/PVA and those loaded with 4, 8, and 12 mL of CuO-NPs, is investigated at room temperature as illustrated in Figures 4 and 5. In Figure 4a, the permittivity of the CMC/PVA composite shows the lowest values compared to those mixed with CuO-NPs. This means that introduction of CuO enhances the composite polarizability. This in fact originated from reducing both porosity volume fraction and the number of porous as reported by SEM results. It is generally reported that the porosity reduces the electrical polarization and thus decreases permittivity [19, 20]. As a result, the porous material is projected to have less polarization than its dense counterpart because it contains fewer active components. Another reason for the porosity-dependent permittivity is as the porous volume fraction increases, the number of electric dipole moments per unit volume decreases, revealing a total polarization decrease, i.e. permittivity decreases. On the other side, the permittivity decreases at a very slow rate upon increasing the frequency and attained much lower values (~ 4 to 5) at high frequency (10^6 Hz). It is well known that as the frequency increases, both the permittivity and loss tangent for most materials decreases due to a decrease in the total polarization components; space charge, dipolar, ionic, and electronic [21, 22]. In view of this, the obtained low permittivity values are expected to be decreased much more within a microwave frequency range (300 MHz-300 GHz). Accordingly, the expected low permittivity values of CMC/PVA-based composites would be promising for high-speed signal transmission with minimum attenuation. Following is a demonstration of this. The relationship between high-frequency signal transmission speed V , signal transmission loss, and the interlayer dielectric material is stated as follows based on the signal transmission rate formula:

$$v = \frac{kc}{\sqrt{\epsilon'}} \quad (4)$$

where k is a constant and V (m/s) and c (m/s) represent the speed of light in a vacuum and the propagation of signals, respectively. According to this formula, signal propagation rates will be faster the lower the permittivity of the dielectric material.

The loss in permittivity represents the electric energy lost by the material as heat or/and leakage current. This loss can be determined by a dielectric property called the loss tangent ($\tan\delta$). The loss tangent value of a

dielectric, however, is another issue to take into account in high-frequency circuits. This study has examined the frequency-dependent loss tangent of CMC/PVA-based composites over a broad frequency range, as shown in Fig. 4b. As clear, $\tan\delta$ increases with increasing CuO-NPs content whereas it decreases rapidly with increasing frequency and attained much lower values (~ 0.0006 to 0.0009) at 10^6 Hz. As suggested above, the obtained loss tangent values are expected to be decreased much more in the high frequency. Thus, CMC/PVA-based composites would be promising in high-frequency applications. This can be demonstrated by the following formula:

$$\alpha = k' f \tan\delta \sqrt{\epsilon'} \quad (5)$$

where α (dB/m) is the signal transmission loss of the dielectric. The attenuation of signal propagation decreases with decreasing loss tangent of the dielectric. The study and development of high-performance dielectric materials with low permittivity and low loss tangent is the foundation of the high-frequency application of CMC/PVA-based composites, it can be inferred from the foregoing.

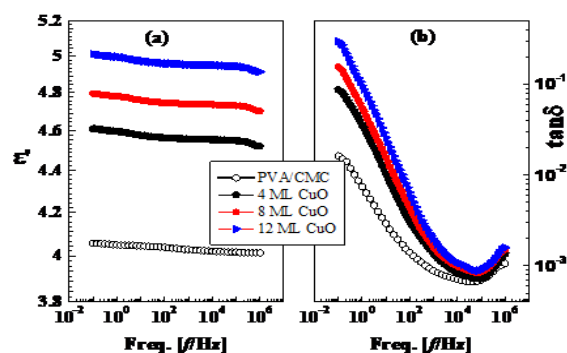


Figure 4: The permittivity (ϵ') and loss tangent ($\tan\delta$), both at room temperature, depending on frequency (f).

The AC conductivity (σ_{ac}) is an also essential property that determines the electrical conduction of material upon applying an alternating electric field [18, 23, 24]. It is mainly dependent on the concentration and mobility of the free charge carriers [25-27]. In the current study, the frequency dependence of σ_{ac} , at room temperature, has been investigated as demonstrated in Figure 5. As clear, σ_{ac} increases with increasing frequency at two different rates below and above 10^3 Hz. It increases relatively with a slow rate below 10^3 Hz, then remarkably increases at higher frequencies, obeying the universal power law ($\sigma_{ac} \propto \omega^s$), where ω is the angular frequency, $0 < s \leq 1$ is the frequency exponent [28]. The hopping of charge carriers in the localized state is what results in

this improvement in conductivity. In general, the term "hopping" refers to the abrupt movement of free charge carriers from one point to another nearby site, which encompasses both quantum mechanical tunneling and hops over a potential obstacle [21]. This is common for polymeric and semiconductor samples. In addition, σ_{ac} exhibits much lower values (10^{-13} S/cm) at very sufficient frequency, reflecting the insulation property of CMC/PVA – based composites. We also notice that σ_{ac} increases with increasing CuO-NPs content and then all curves merge at frequencies higher than 10^3 Hz.

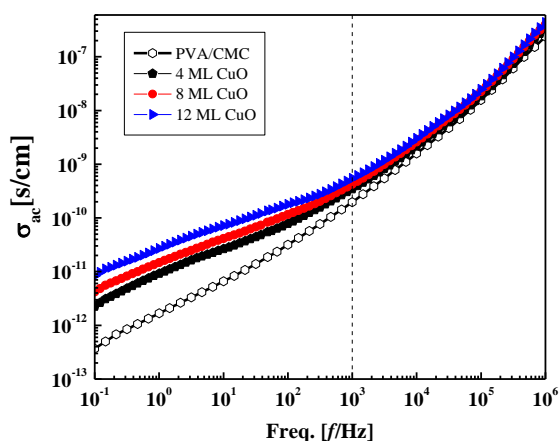


Figure 5: The AC conductivity (σ'_{ac}) at room temperature and its dependency on frequency (f)

4. Conclusions

Preparation of a floating membrane using polyvinyl alcohol (PVA), carboxymethyl cellulose (CMC) polymer, and copper oxide (CuO) for water desalination was carried out. The produced floating membrane was found to effectively evaporate water from the saline solution. The optimization of the efficiency of the produced membrane by using different nanomaterials as well as different concentrations of nanomaterials incorporated with the polymer used for manufacturing the floating membrane is of vital importance.

On the basis of dielectric data collected for CMC/PVA/CuO composites, we have drawn the following conclusions:

- Both permittivity and loss tangent decreased with increasing frequency whereas they slightly increased with increasing CuO-NPs content. AC conductivity increased with increasing both frequency and CuO-NPs content. Further, it showed much lower values (10^{-13} S/cm), reflecting insulation property of all composites.

- Interestingly, the low permittivity (~ 4 to 5) and loss tangent (~ 0.0006 to 0.0009) values make CMC/PVA/CuO composites promising for high-speed signal transmission with minimum attenuation. The interesting features of these composites make them technologically important and competitive to other alternative materials, not only due to their low loss and permittivity values but also due to their cost-effectiveness.

5. Conflicts of interest

“There are no conflicts to declare”.

6. Formatting of funding sources

This research work has been carried out within the framework of a project financed by the National Research Centre “E 120805”.

7. References

1. Gao, M., et al., *Solar absorber material and system designs for photothermal water vaporization towards clean water and energy production*. Energy & Environmental Science, 2019. **12**(3): p. 841-864.
2. Frascari, D., et al., *Integrated technological and management solutions for wastewater treatment and efficient agricultural reuse in Egypt, Morocco, and Tunisia*. Integrated environmental assessment and management, 2018. **14**(4): p. 447-462.
3. Ammar, N., et al., *Wollastonite ceramic/CuO nano-composite for cadmium ions removal from waste water*. Egyptian Journal of Chemistry, 2017. **60**(5): p. 817-823.
4. Wahba, S.M., K. Scott, and J.K. Steinberger, *Analyzing Egypt's water footprint based on trade balance and expenditure inequality*. Journal of Cleaner Production, 2018. **198**: p. 1526-1535.
5. El-Khateeb, M., et al., *ENVIRONMENTAL POLLUTION PREVENTION VIA HEAVY METAL REMOVAL*. Waste Management and Utilization Techniques: p. 17.
6. El-Khateeb, M.A., et al., *Polishing of secondary treated wastewater using nano-ceramic hybrid PET waste plastic sheets*. Desalin. Water Treat, 2021. **217**: p. 214-220.
7. El-Khateeb, M. and F. El-Gohary, *Combining UASB technology and constructed wetland for domestic wastewater reclamation and reuse*.

- Water Science and Technology: Water Supply, 2003. **3**(4): p. 201-208.
8. Zhu, L., et al., *Solar-driven photothermal nanostructured materials designs and prerequisites for evaporation and catalysis applications*. Materials Horizons, 2018. **5**(3): p. 323-343.
 9. Zhu, L., et al., *Dual-phase molybdenum nitride nanorambutans for solar steam generation under one sun illumination*. Nano Energy, 2019. **57**: p. 842-850.
 10. Irshad, M.S., N. Arshad, and X. Wang, *Nanoenabled photothermal materials for clean water production*. Global Challenges, 2021. **5**(1): p. 2000055.
 11. Zhang, P., et al., *Direct solar steam generation system for clean water production*. Energy Storage Materials, 2019. **18**: p. 429-446.
 12. Wilson, H.M., et al., *Ultra-low cost cotton based solar evaporation device for seawater desalination and waste water purification to produce drinkable water*. Desalination, 2019. **456**: p. 85-96.
 13. Bazli, L., et al., *Correlation between viscoelastic behavior and morphology of nanocomposites based on SR/EPDM blends compatibilized by maleic anhydride*. Polymer, 2017. **113**: p. 156-166.
 14. Wu, X., et al., *A flexible photothermal cotton-CuS nanocage-agarose aerogel towards portable solar steam generation*. Nano energy, 2019. **56**: p. 708-715.
 15. Dao, V.D. and H.S. Choi, *Carbon-based sunlight absorbers in solar-driven steam generation devices*. Global Challenges, 2018. **2**(2): p. 1700094.
 16. Ebin, B., O. Gencer, and S. Gurmen, *Aerosol Route Synthesis of Copper Oxide Nanoparticles Using Copper Nitrate Solution*. 2010, Minerals, Metals and Materials Society/AIME, 420 Commonwealth Dr., P. O. Box
 17. Kremer, F. and A. Schönhal, *Broadband dielectric spectroscopy*. 2002: Springer Science & Business Media.
 18. Zhu, L., et al., *Recent progress in solar-driven interfacial water evaporation: advanced designs and applications*. Nano Energy, 2019. **57**: p. 507-518.
 19. Wagner, K.W., *Erklärung der dielektrischen nachwirkungsvorgänge auf grund maxwellscher vorstellungen*. Archiv für Elektrotechnik, 1914. **2**(9): p. 371-387.
 20. Ma, Y., et al., *Tunable dielectric and other properties in high-performance sandwich-type polyimide films achieved by adjusting the porous structure*. Journal of Materials Chemistry C, 2019. **7**(24): p. 7360-7370.
 21. Hashim, A. and A. Hadi, *Novel pressure sensors made from nanocomposites (biodegradable polymers-metal oxide nanoparticles): fabrication and characterization*. Ukrainian Journal of Physics, 2018. **63**(8): p. 754-754.
 22. Giesbrecht, P.K. and M.S. Freund, *Recent advances in bipolar membrane design and applications*. Chemistry of Materials, 2020. **32**(19): p. 8060-8090.
 23. El-Sayed, S. and A. El Sayed, *Preparation and Characterization of CuO/Co3O4/Poly (Methyl Methacrylate) Nanocomposites Films for Optical and Dielectric Applications*. 2021.
 24. Jlassi, I., N. Sdiri, and H. Elhouichet, *Electrical conductivity and dielectric properties of MgO doped lithium phosphate glasses*. Journal of Non-Crystalline Solids, 2017. **466**: p. 45-51.
 25. Ding, T., et al., *Hybrid solar-driven interfacial evaporation systems: Beyond water production towards high solar energy utilization*. Materials Today, 2021. **42**: p. 178-191.
 26. Atta, M., et al., *Enhanced optical, morphological, dielectric, and conductivity properties of gold nanoparticles doped with PVA/CMC blend as an application in organoelectronic devices*. Journal of Materials Science: Materials in Electronics, 2021. **32**(8): p. 10443-10457.
 27. Jonscher, A., *Physics of Thin Films, ed. by MH Francombe*. 1980, Academic Press, London, New York.
 28. Zhang, C., et al., *Harnessing solar-driven photothermal effect toward the water-energy nexus*. Advanced Science, 2019. **6**(18): p. 1900883.